ASYMMETRICAL PMUTS FOR FOCUSED ACOUSTIC PRESSURE BY REINFORCEMENT LEARNING

Wei Yue[1,†], Fanping Sui[1,†], Yande Peng[1], Fan Xia[1], Peggy Tsao[1], Megan Teng[1], Hanxiao Liu[2], and Liwei Lin[1,2]

[1]Department of Mechanical Engineering, University of California, Berkeley, USA
[2]Tsinghua-Berkeley Shenzhen Institute, Tsinghua University, Shenzhen, China
[†]Wei Yue and Fanping Sui contributed equally to this work.

ABSTRACT

To increase the energy utilization of a pMUT array, an advanced design scheme for asymmetrical piezoelectric micromachined ultrasonic transducers (pMUTs) has been developed with focused acoustic pressure via the deep deterministic policy gradient (DDPG) algorithm. Three distinctive accomplishments have been achieved in: 1) a highly-efficient interface platform between Python and COMSOL for asymmetry factor (AF) simulations; 2) fast freeform pMUT designs without the initial dataset; and 3) superior designs with increased 34% pressure outputs for potential applications such as contact-less haptics. As such, the proposed design scheme could be applied to other MEMS devices to improve system efficiency.

KEYWORDS

Machine Learning, Piezoelectric Micromachined Ultrasonic Transducer, Asymmetry Factor, Deep Reinforcement Learning.

INTRODUCTION

PMUT arrays have shown promising applications in various fields, such as 3D-ranging [1], haptic interfaces [2], fingerprint sensing [3], … etc. In the state-of-art pMUT designs, identically PMUT elements are arranged in an array to enhance the acoustic pressure profile. This setup often results in low acoustic pressue without using control mechanisms such as beam forming to assist and focus the outputs. In large scale systems, bulky acoustic transducers are often placed on a curved surface as an array format to efficiently use the acoustic pressure distributions in the 3D space. This scheme is generally not possible for pMUTs with small form-factors on a flat silicon wafer. This work proposes to change the shape of individual pMUT elements in an array setup to generate asymmetrical pressure outputs and to focus the acoustic energy for enhanced outputs.

Previously, machine learning techniques have shown reliable and efficient results in the design of Micro-Electro-Mechanical Systems (MEMS) [4], especially in geometric-related problems. Supervised learning, in particular, has been widely used by collecting large amounts of data to train a predictive model. However, even with a perfect predictive model, it is impossible to perform inverse design or design optimization because the model can only predict performances based on a given design geometry and it cannot generate specific geometries with desired properties. To address this issue, the supervised learning scheme is combined with other optimization algorithms, such as the genetic algorithms [5]. While simulations are convenient to

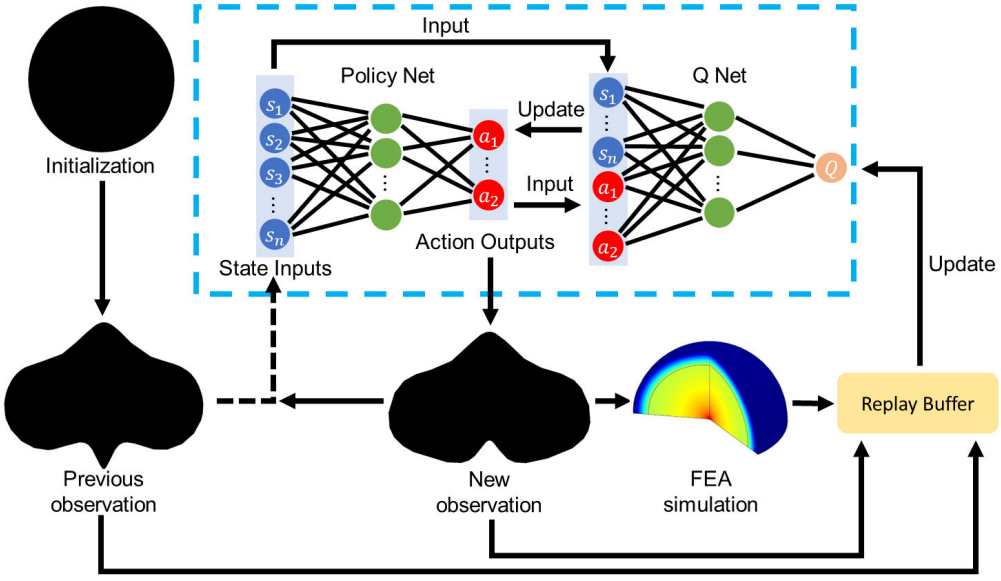

Figure 1: Overall flow chart of the proposed optimization framework. In each episode, the geometry will be initialized as a circle at first. The policy will suggest an action to change the feature according to the current state. The new geometry will be evaluated by FEA to calculate the asymmetry factor. By adding the current and new geometry, action, and reward to the replay buffer for training, the Q net for reward estimation and the policy net will be updated for better accuracy.

generate data, it is time-consuming to randomly generate a dense dataset in the entire design space. For example, it is unnecessary to learn data pointsfar from desired properties. Deep reinforcement learning (DRL) is a widely utilized technique in AI as it offers better options for inverse design problems. Unlike supervised learning, the agent in DRL can access the simulation environment during the training process, allowing it to find the most useful data points. By exploring and training simultaneously, a policy for the best objective is quickly established to eliminate the need to combine other optimization methods.

In this study, we present a novel deep reinforcement learning (DRL) framework that utilizes the deep deterministic policy gradient (DDPG) algorithm [6] for the design optimization of highly asymmetrical pMUTs. This proposed framework requires no prior knowledge and can iteratively interact with COMSOL simulation environment to generate new data points automatically. An interface platform has been constructed between Python and COMSOL to enable the seamless operation of the process. After about 250 episodes of exploration and training, a well-behaved feature-changing policy is established, resulting in well-performed designs. This framework offers a powerful alternative to enhance the optimization process, opening up new avenues for MEMS designs.

SYSTEM ARCHITECTURE

Fig. 1 depicts the fully automated and DRL-based optimization flow chart. Each optimization cycle begins with a circular shape pMUT and progresses by sequentially adjusting the coordinates of key points to determine the diaphragm shape. The closed interpolation curve of all key points guarantees smoothness, and all coordinates of key points are located in a continuous feasible domain, requiring continuous actions to represent key point changes. To accomplish non-discrete geometric feature changes, two deep neural networks, a policy network, and a critic network (Q network), are used synergistically. The Q-value predicted by the critic network estimates the final asymmetry factor (AF) after each optimization episode to give a certain pair of action and state. In discrete problems, the best action is easily determined by comparing Q-values. For continuous problems, however, infinite possibilities make direct comparison impossible. The policy network resolves this by taking the current state as input and outputting the suggested feature-changing action, providing optimal action choices throughout the space. Each step is determined by the policy net's feature-changing policy. The reward for each step, representing the variation of the AF, is measured via finite element analysis (FEA) in COMSOL. The FEA involved two distinct steps: the resonance frequency detection step and the acoustic field simulation step. To ensure that pMUTs with different shapes have the same resonance frequency (50 kHz in this study), their shapes will be scaled based on the original resonance frequency obtained from the first step. Subsequently, at the desired frequency, a multi-physical simulation will be performed to analyze the AF. The current and new geometry, action, and reward are collected in the replay buffer to update the critic network and policy network with stochastic gradient descent (SGD) for more accurate long-term reward predictions. After enough

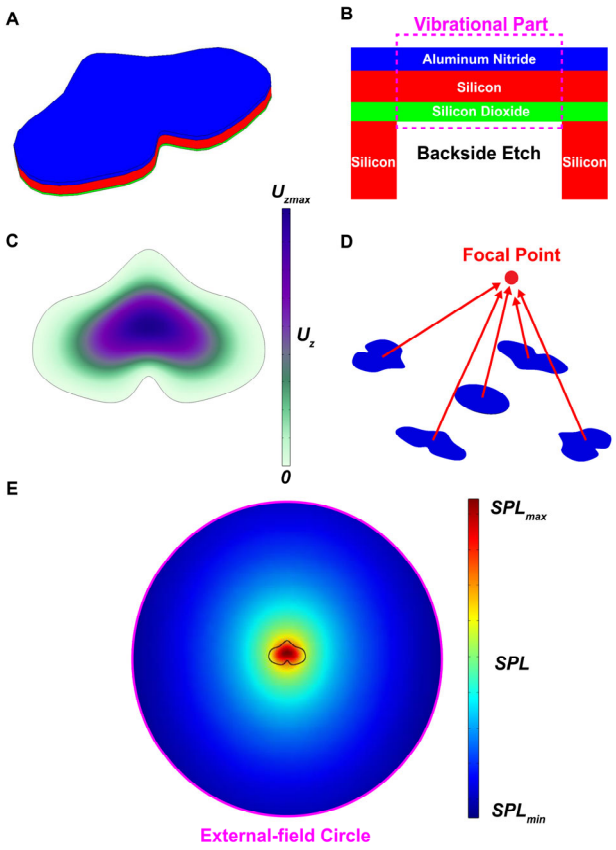

*Figure 2: **A**) Geometry of a representative pMUT. **B**) cross sectional schematic of the pMUT. The thickness for the silicon dioxide layer, silicon layer and aluminum nitride layer is 1 μm, 5 μm and 2 μm, respectively. **C**) The mode shape of a representative pMUT. **D**) The arrangement of different pMUTs in an array. The peripheral pMUTs result in the asymmetrical pressure output to increase the energy utilization. **E**) The sound pressure level of the representative pMUT. The plane is 0.1 m above the pMUT.*

training steps, the optimal pMUT design is obtained when the policy net and critic net make the best choice and accurately estimate the reward.

Fig. 2A illustrates a design example of the pMUT diaphragm composed of three layers: the thin SiO2 layer (green), the thick inactive Si layer (red), and the active piezoelectric AlN layer (blue). This diaphragm functions as the vibrational structure defined by the backside etching process, as shown in the cross-sectional view in **Fig. 2B**. The boundaries of the three layers are fixed to the silicon substrarte. PMUTs with complex membrane shapes can be designed to produce different vibrational patterns, such as an example shown in **Fig. 2C**. The deformation of the diaphragm follows its shape as a heart-like contour in this case and this asymmetrical design will generate a resulting asymmetrical acoustic field to exert stronger pressure in certain directions. The acoustic field of this heart-like pMUT structure has been simulated in COMSOL. The sound pressure level (SPL) distribution 0.1 m away from the diaphragm surface is demonstrated in **Fig. 2E**. In this case, the SPL contour exhibits the egg-like shape with higher pressure outputs in the upper half. To quantify this result, the average SPL difference between the upper and

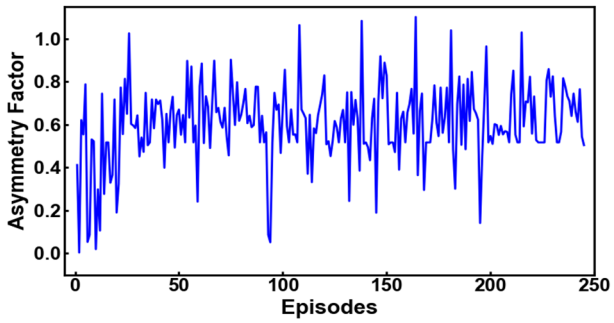

Figure 3: Asymmetry factors with respect to the number of episodes. In the initial 20 episodes, the agent randomly explores the design space. After that, the training and exploration proceed simulataneously. With 50 episodes, a design with AF over 1 is found.

lower halves of the external-field circle far away from the pMUT is defined as the asymmetry factor (AF). Since the directionality in the far-field barely changes with distance, the radius of the external-field circle is not critical. In this work, the radius is fixed at 0.1 m for each pMUT. Due to the non-uniform energy distribution generated by the asymmetrical pMUT designs, the output pressure can be analyzed accordingly. When the target focal point of the ultrasound pressure is not directly above a single pMUT in an array setup, as shown in **Fig. 2D**, the asymmetrical pMUT designs can increase energy utilization as compared to that of using only circular-shape pMUTs without using the conventional scheme of phase differences of individual pMUTs for beam-forming operaitons. Specifically in this case, the heart-like pMUTs can increase the energy utilization by ~8% as compared to that of the same array by using only circular-shape pMUTs. Specifically, for a large array structure composed of only circular-shape pMUTs, the peripheral ones have low contributions to the focal point pressure. Therefore, it is desirable to construct asymmetrical pMUTs in the array format with large AF to increase the energy utilization.

RESULTS AND DISCUSSION

To validate the credibility of the simulation results, the parameters are set to be identical to those in a prior work with comparison results in **Table 1**. A strong agreement is observed between the simulation and experimental data as the validation of our simulations.

Table 1: Simulated and experimental SPL data of an AlN circular pMUT for validation. [7]

	Experimental Results	Simulation in this work
SPL with 2 V Voltage Amplitude (dB)	107.0	107.5
SPL with 4 V Voltage Amplitude (dB)	113.1	113.5

The learning curve in **Fig. 3** exhibits progressive increases in AF as the training process advances. To prevent the algorithm being trapped in local minimums, noises are introduced in accordance with the decaying exploration parameter, which compels the policy to study

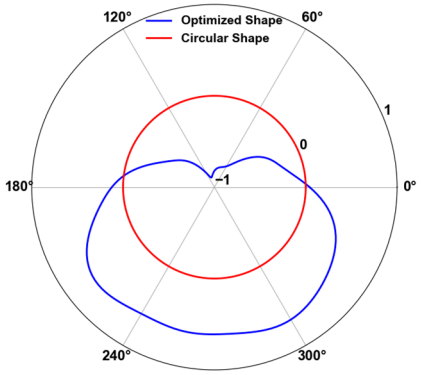

Figure 4: The normalized SPL configurations after the optimization process (blue line) based on a circular-shape pMUT (red line) at the external-field circle. The circular-shape pMUT has the fixed SPL at 0 dB for all directions. In contrast, the SPL generated by the optimized pMUT shows strong asymmetry with a strongest SPL at 270° for 0.68 dB, and a weakest SPL at 90° for -0.89 dB.

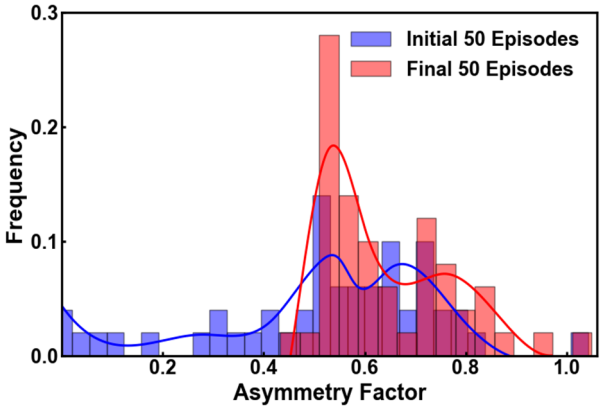

Figure 5: Asymmetry factor distributions of the initial and final 50 episodes. A significant difference can be observed, showing the performance of the optimization process.

unexplored designs. Additionally, during the initial 20 episodes, the policy solely performs exploration without learning to enrich the relay buffer and establish a relatively random design space. Afterward, the policy learns and explores simultaneously to comprehend the design scheme. After 50 episodes, exceptional designs with AF above 1 are discovered. As the level of randomness decreases, the agent converges to a neighborhood of the optimal design.

Fig. 4 shows the sound pressure level (SPL) distributions on the external circle for the optimized pMUT with an AF of 1.102 and that of a circular pMUT. The SPL results have been normalized to ensure comparability, and a strong asymmetry is observed for the optimized design. The strongest SPL at 270° is 0.68 dB, while the weakest SPL at 90° is -0.89 dB, resulting in a difference of 1.57 dB or a pressure difference of 34%. On average, the SPL difference between the upper and lower halves of the external circle is 1.102 dB or a pressure difference of 14%. In other words, there is 30% more energy distributed in the lower half of the circle than that in the upper half.

Fig. 5 depicts the AF distributions for the starting designs of the initial 50 episodes and the optimized designs for the last 50 episodes. The starting designs exhibit a relatively uniform distribution, with a large number of designs in the region below the AF value of 0.4. The lowest AF among the starting designs is 0.003, indicating almost no asymmetry. In contrast, the optimized designs show a significant improvement, with the lowest AF value of 0.45. This indicates that the feature-changing policy is effective in finding designs with high AF. On average, the optimized designs have an AF of 0.642, or a ~22% increase compared to that of starting designs with an average AF of 0.525.

Fig. 6A lists representative optimized design. Notably, the spindle-like shape has a significantly large AF, which can be qualitatively explained. First, the spindle-like shape undergoes horizontal shrinkage and vertical extension, concentrating most of the energy near the symmetrical axis. Second, the thin tip at the bottom serves as an effective boundary to limit the output from this part. In contrast, the inferior designs in **Fig. 6B** differ from the optimized designs. Some of them have symmetrical shapes, while others have similar dimensions in vertical and horizontal directions. These comparisons are important for future designing guidances.

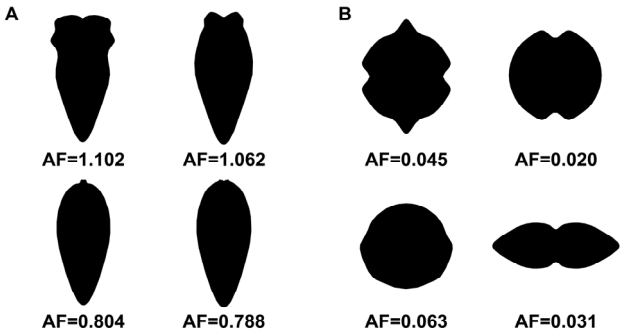

*Figure 6: **A)** Optimized geometric patterns. **B)** Inferior geometric patterns. A spindle-like shape is observed in all optimized designs, which can be used as an important design guidance.*

CONCLUSION

This study utilizes a novel deep reinforcement learning (DRL)-based framework to design asymmetrical pMUTs in the array setup for optimize acoustic pressure outputs. The pMUT geometry is transformed into coordinates of key points, which are used as the input to the neural network. At each step, the policy suggests a feature-changing action based on the current geometry. The newly generated design is then analyzed using FEA to evaluate its performance, which serves as training data to update the policy. Through adequate exploration and training, the policy learns to generate good designs by comprehending the rules. The optimized pMUT designs show significant improvement in acoustic output utilizations for potential pMUT array applications. Therefore, the proposed DRL-based framework offers an effective alternative for MEMS design problems to significantly reduce the time required for the data preparation and numerical simulation process. Future works may use more advanced algorithms, such as the Soft Actor-Critic (SAC) [8] or Proximal Policy Optimization (PPO) [9] to further enhance the efficiency.

ACKNOWLEDGEMENTS

The authors appreciate the helpful discussions with Professor Grace X. Gu, Dr. Renxiao Xu and Dr. Ruiqi Guo. The work is partially supported by Berkeley Sensor and Actuator Center and NSF grant - ECCS- 2128311.

REFERENCES

[1] H. Liu, Y. Peng, W. Yue, S. Umezawa, S. Ikeuchi, Y. Aida, C. Chen, P. Tsao, L. Lin, "Drone-Mounted Low-Frequency pMUTS for > 6-Meter Rangefinder in Air", in *2023 IEEE 36th International Conference on Micro Electro Mechanical Systems (MEMS)*, Munich, Germany, 2023, pp. 957-960.

[2] W. Yue, Y. Peng, H. Liu, F. Xia, F. Sui, S. Umezawa, S. Ikeuchi, Y. Aida, L. Lin, "Auto-Positioning and Haptic Stimulations via A 35 mm Square Pmut Array", in *2023 IEEE 36th International Conference on Micro Electro Mechanical Systems (MEMS)*, Munich, Germany, 2023, pp. 941-944.

[3] X. Jiang, H. Tang, Y. Lu, E. J. Ng, J. M. Tsai, B. E. Boser, D. A. Horsley, "Ultrasonic fingerprint sensor with transmit beamforming based on a PMUT array bonded to CMOS circuitry", *IEEE Trans. Ultrason. Ferroelectr. Freq. Control.*, vol. 64, pp. 1401-1408, 2017.

[4] R. Guo, F. Sui, W. Yue, Z. Wang, S. Pala, K. Li, R. Xu, L. Lin, "Deep learning for non-parameterized MEMS structural design", *Microsyst. Nanoeng.*, vol 8, pp. 91, 2022.

[5] F. Sui, W. Yue, R. Guo, K. Behrouzi, L. Lin, "Designing Weakly Coupled Mems Resonators with Machine Learning-Based Method", in *2022 IEEE 35th International Conference on Micro Electro Mechanical Systems Conference (MEMS)*, Tokyo, Japan, 2022, pp. 454-457.

[6] D. Silver, G. Lever, N. Heess, T. Degris, D. Wierstra, M. Riedmiller, "Deterministic policy gradient algorithms", in *Proceedings of the 31st International Conference on Machine Learning*, PMLR, 2014, pp. 387-395.

[7] Z. Shao, S. Pala, Y. Peng, L. Lin, "*Bimorph pinned piezoelectric micromachined ultrasonic transducers for space imaging applications*", *J. Microelectromechanical Syst.*, vol 30, pp. 650–658, 2021.

[8] T. Haarnoja, A. Zhou, P. Abbeel, S. Levine, "Soft actor-critic: Off-policy maximum entropy deep reinforcement learning with a stochastic actor", in *Proceedings of the 35th International Conference on Machine Learning*, PMLR, 2018, pp. 1861-1870.

[9] J. Schulman, F. Wolski, P. Dhariwal, A. Radford, O. Klimov, "Proximal policy optimization algorithms", *arXiv preprint* arXiv:1707.06347, 2017.

CONTACT

*W. Yue; +1-510-984-8328; wei_yue@berkeley.edu
*F. Sui; +1-341-333-9262; fpsui@berkeley.edu